ORIGINAL ARTICLE

Experimental analysis of concrete flat slabs with internal stud-type shear reinforcement

Análise experimental de lajes lisas de concreto armado com armadura de cisalhamento do tipo stud interno

Diego Borja Ferreira[a,b] [ID]
Leandro Mouta Trautwein[a] [ID]
Jeovan Pereira das Virgens[a,c] [ID]
Ronaldo Barros Gomes[c] [ID]
Luiz Carlos de Almeida[a] [ID]

[a]Universidade Estadual de Campinas – UNICAMP, Engenharia Civil, Campinas, SP, Brasil
[b]Instituto Federal de Educação Ciências e Tecnologia, Engenharia Civil, Cidade de Goiás, GO, Brasil
[c]Universidade Federal de Goiás – UFG, Engenharia Civil, Goiânia, GO, Brasil

Abstract: This study evaluates seven flat slabs made with reinforced concrete. There are three reference slabs, one of them doesn't present any shear reinforcement. Four slabs have a new model of shear reinforcement of stud type, internally anchored to the flexural reinforcements. That reinforcement has an additional element, called on this study by the name: anti-cracking pins. The main objective of the research is to find the ideal spacing between these pins to achieve a failure mode and a failure load similar to the reference slabs that have conventional studs. For that, are evaluated: vertical displacements, rotation, shear reinforcement deformation, load capacity and failure mode. The slabs with the new stud have a load gain of 40% to 106% compared to the slab without studs LRef. The slab L-5-13 presented a load and a failure mode similar to the slab of reference, LRef-AC.

Keywords: flat slab, punching, shear reinforcement.

Resumo: Esse estudo avalia sete lajes lisas de concreto armado. São três lajes de referência, dessas uma não apresenta armadura de cisalhamento, e quatro com uma novo modelo de armadura de cisalhamento do tipo stud, ancorado internamente às armaduras de flexão. Essa armadura possui um elemento adicional, denominado nessa pesquisa de pinos anti-fissuração. O objetivo principal da pesquisa é encontrar o espaçamento ideal entre esses pinos para atingir um modo e carga de ruptura semelhante às lajes de referência com studs convencionais. Para tanto são avaliados deslocamentos verticais, rotação, deformação das armaduras de cisalhamento, capacidade de carga e modo de ruptura. As lajes com o novo stud apresentam ganho de carga de 40% a 106% com relação à laje sem studs LRef. A laje L-5-13 apresentou carga e modo de ruptura similar à sua laje de referência LRef-AC.

Palavras-chave: lajes lisas, punção, armadura de cisalhamento.

1 INTRODUCTION

The use of flat slabs made with reinforced concrete is standing out in civil engineering due to its advantages in the construction process. The absence of beams reduces cuts in the production process of formwork. Therefore, it reduces

D. B. Ferreira, L. M. Trautwein, J. P. Virgens, R. B. Gomes, and L. C. Almeida

costs and rationalizes construction. The increased flexibility in the conception of projects for building and architectural installations is also a possibility in the use of this slab model.

As any structural system, the use of flat slabs must take into account some unfavorable aspects. The large vertical displacements presented by this structural model points to the use of elements that increase its stiffness [1].

Another preponderant factor in the use of this type of slab concerns to the punching effects in the columns area. The high concentration of shear forces can lead the structural element to collapse. Figure 1 shows the loaded region, it is possible to observe the development of cone-shaped cracking around the columns, the use of mechanisms can minimize these effects.
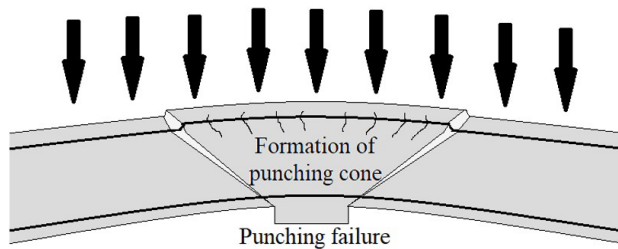
Figure 1: Failure by punching.

One of the possibilities to minimize the punching effects is to increase the concrete cross section in the region of the connection with the columns, but this technique causes problems in the architectural project. Another technique to combat this effect is the use of reinforcement, is the most efficient method to increase the capacity and ductility of flat slabs [2], [3].

The use of shear reinforcement to combat punching effects can lead to three distinct failure modes: failure by crushing of the compression strut near the column face (Figure 2a); failure by yielding of the shear reinforcement in the internal region of the reinforcement (Figure 2b); failure outside the region of the shear reinforcement with characteristics similar to the failure of slabs without shear reinforcement (Figure 2c), [2].
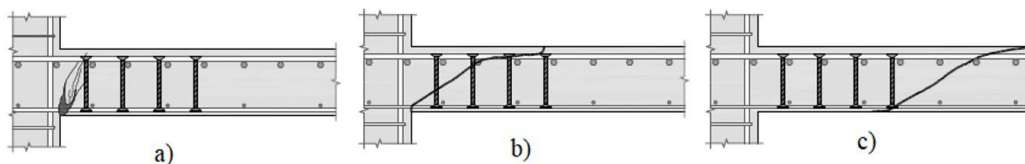
Figure 2: Crack patterns [4]

Several studies [1], [5]–[8], used internal-type shear reinforcement point to a specific type of failure called delamination, in which the failure surface touches the bases of the reinforcement (Figure 3) anticipating collapse.

Figure 3: Crack delamination patterns.

The work in question presents a comparative study of flat slabs investigating the effects of two models of stud-type shear reinforcement, which differ in terms of anchorage in the flexural reinforcement (Figure 4). The structural performance was evaluated by analyzing the strength and stiffness, as well as possible the benefits in the mounting process in the construction environment.
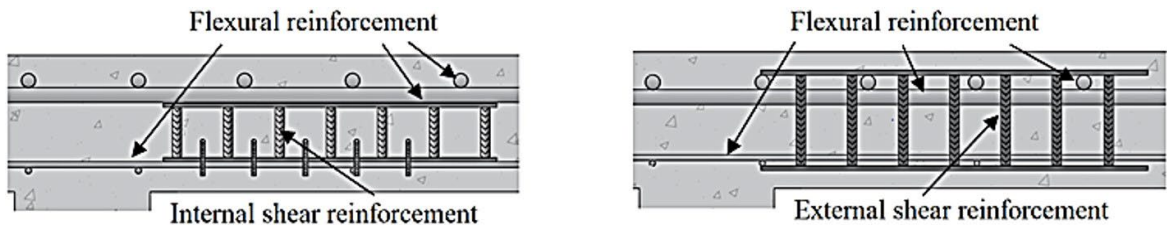
Figure 4: Shear reinforcement with different anchorage types.

2 EXPERIMENTAL PROGRAM

The experimental program reproduced a reinforced concrete panel with a central column with side dimensions 150mm x 150mm, simulating the behavior of punching effects in flat slabs.

The experimental analysis was made through tests until the failure of seven square flat slabs with 2400 mm side and 150 mm thick, with a flexural reinforcement ratio sufficient to prevent failure by this reinforcement. All slabs have the same characteristics varying only the shear reinforcement.

2.1 Characteristics of the slabs

The study is composed by a reference slab that has no shear reinforcement named LRef, two slabs with conventional stud-type shear reinforcement with external anchorage in the flexural reinforcement, named LRef-AC and LRef-AC-I and four other slabs with a new proposal of stud-type shear reinforcement anchored internally in the flexural reinforcement, named L-5-13, L-5-6, L-5-13-I and L-5-6-I. The slabs with studs that are identified with "I" have internal failure prediction for the current standards and the others, external failure prediction.

Figure 5 shows the slab models tested and Figure 6 shows the details of the studs distribution.
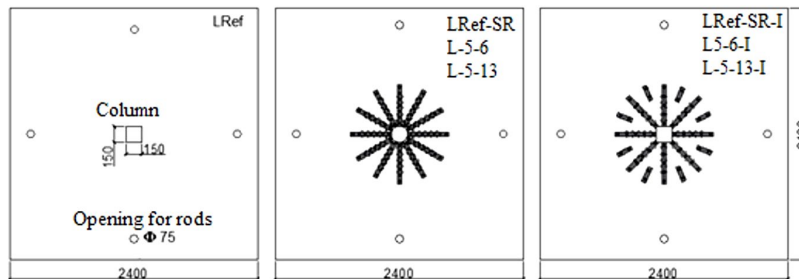
Figure 5: Distribution of studs and reference slab LRef.
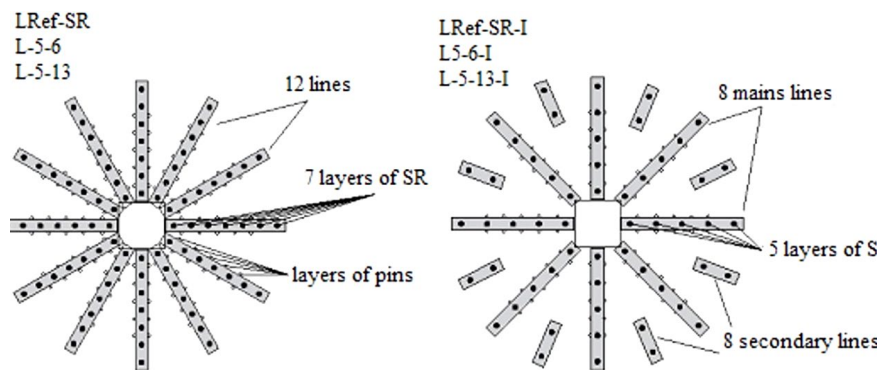
Figure 6: Detail of the stud distribution.

The new stud proposal is based on previous researches [9], [10] that presented excellent results for the use of shear reinforcement anchored internally on the flexural reinforcement. The authors identified some fragility regarding the

development of cracks, noting the appearance of horizontal cracks that tangent the bases of the reinforcement causing a decrease in the ultimate strength.

The slabs L-5-13, L-5-6, L-5-13-I and L-5-6-I use a proposal of internal stud, which have an auxiliary reinforcement in order to minimize the effects of the cracking, this reinforcement has an inverted "U" shape called anti-cracking pin, welded to the bottom plate of the pieces.

In order to neutralize the effects of exudation which can weaken the concrete in the region of the bottom plate, openings of 8 mm in diameter were made – it also contributes to the anchoring of the material. The details of this type of stud can be seen in Figure 7.
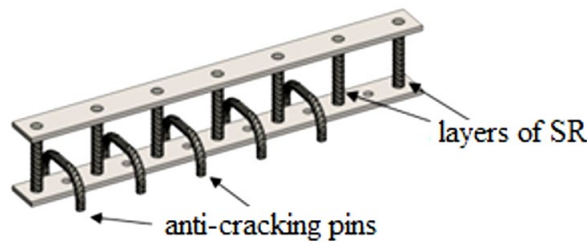
Figure 7: Internal stud model used.

The slabs LRef-AC, L-5-13 and L-5-6 were reinforced due to the prediction of external failure, being composed by 12 lines of studs with 7 layers of shear reinforcement of 10 mm diameter. The slabs LRef-AC-I, L5-13-I and L-5-6-I were reinforced due to the internal failure prediction, consisting in 8 lines of studs with 5 layers of shear reinforcement of 6.3 mm diameter.

The slabs with internal studs have 13 and 6 layers of 5.0 mm anti-cracking pins. The location for using these pins has been defined considering that [1] concluded that the use of pins similar to the one used in this research were efficient in covering the control perimeter region C' defined by NBR 6118 [11] as 2d of the column face. Figure 8 shows the details of the shear reinforcement used in the research.
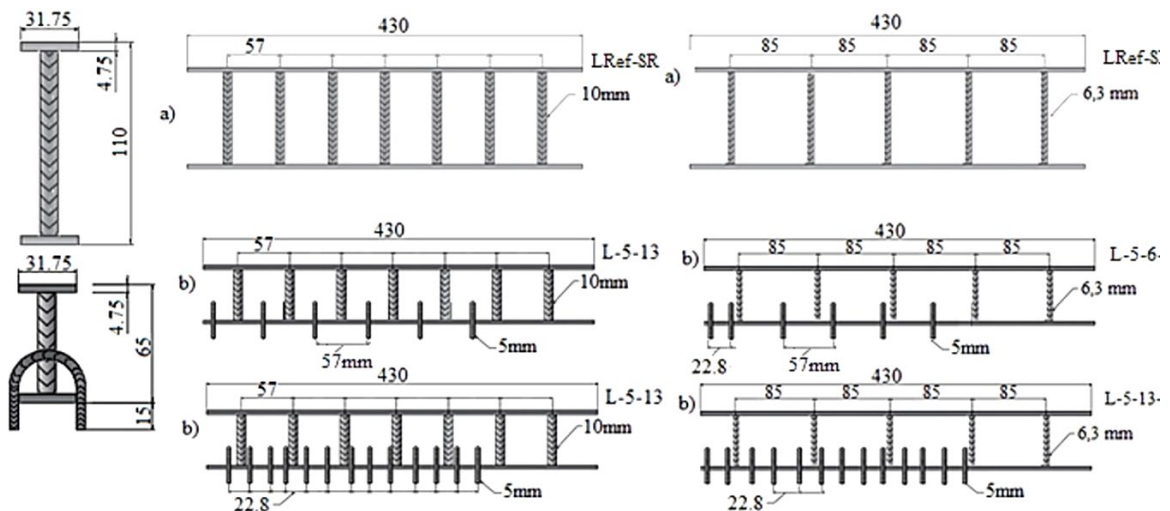
Figure 8: Models of studs.

To combat the effects of flexural forces the slabs were reinforced with 40 straight bars with 16.0 mm diameter of CA-50 steel distributed in cross on the top face and 20 bars with 6.3 mm diameter distributed in cross on the bottom face. In order to increase the anchorage of the bars, 10.0 mm diameter hooks were installed at the slabs ends. The details of the flexural reinforcement are shown in Figure 9.
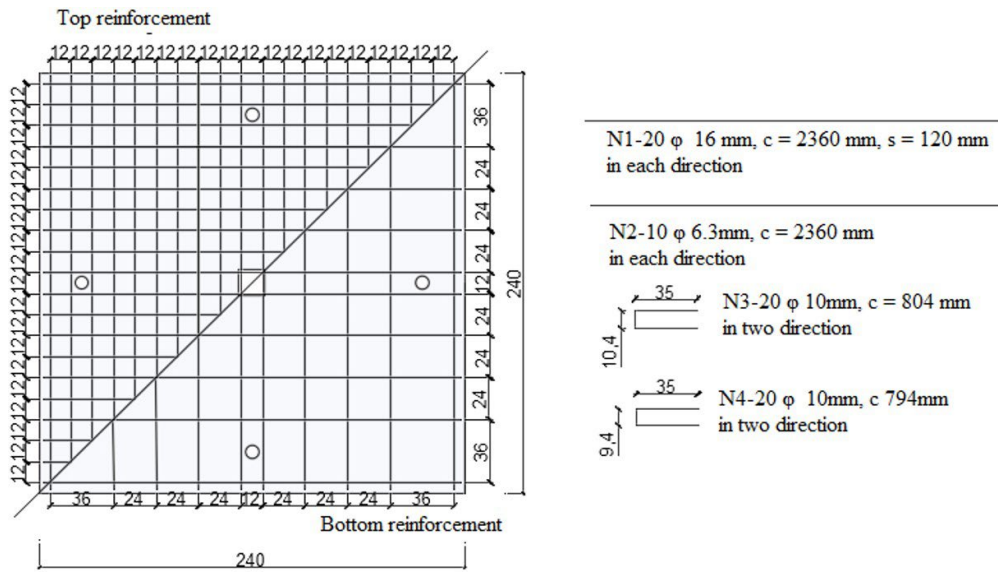
Figure 9: Detailing of the flexural reinforcement.

Conventional studs make it difficult to position bending and shear reinforcement with the ideal spacing foreseen in the design due to the dense amount of reinforcement required in this region, as can be seen in the slabs analyzed by [1], [6], [8] and [12] presented in Figure 10.
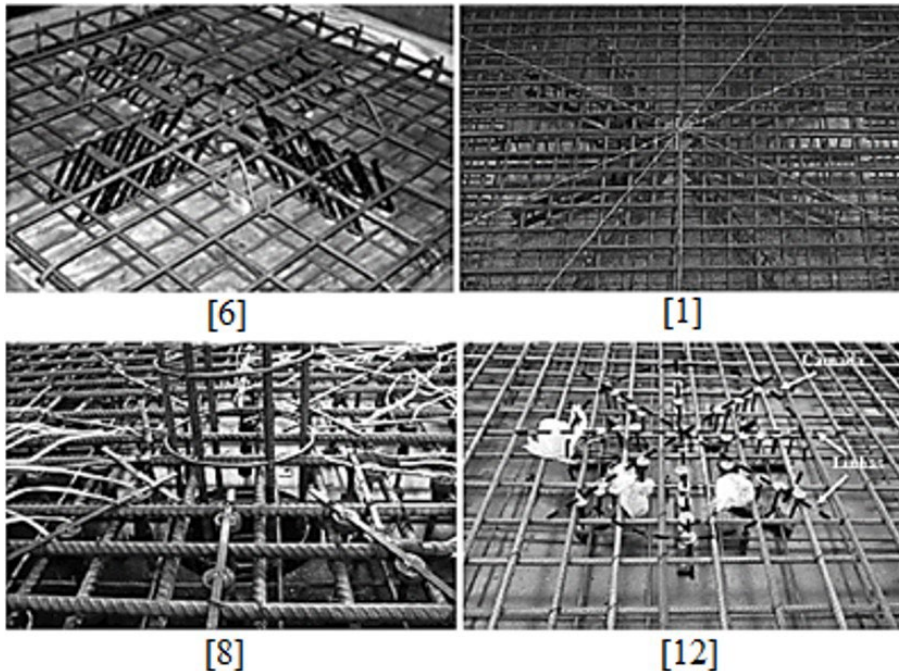
Figure 10: Flexural reinforcements in the region of the slab-column connection.

The use of internal studs presents an advantage in the assembly process, since there is no need to pass the bending bars between the shear reinforcements, which was observed during the assembly of the slabs in this research [1].

The slab reinforcement procedure occurred in the following order: positioning of the bottom bending reinforcement grid (compressed), radial positioning of the studs with the proper angles, positioning of the upper bending reinforcement grid (tensioned), closing with lateral hooks. The reinforcement installing procedure is shown in Figure 11.
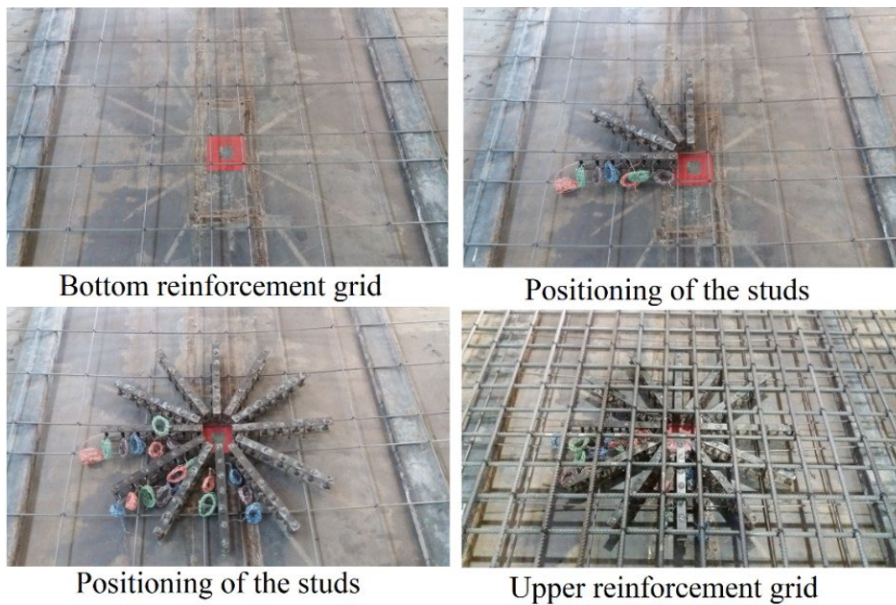
Figure 11: Installing the slab's reinforcement

2.2 Test system

The loading system was set up simulating an internal column, using a hydraulic actuator with capacity of 1000 kN positioned at the bottom of the slab, applying load on a square metal plate of 150 mm side simulating a column, between the plate and the actuator was positioned a load cell to measure the applied load (Figure 12).
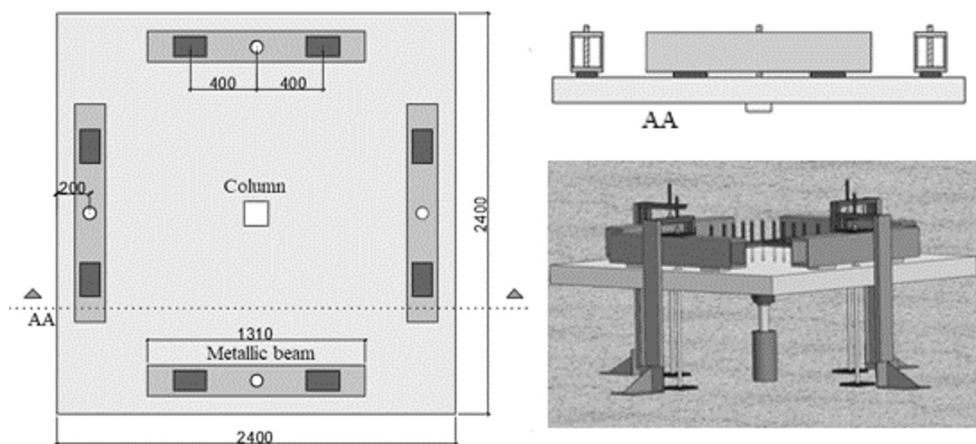
Figure 12: Test system.

3 RESULTS AND DISCUSSIONS

3.1 Load and failure mode

The load obtained by the load cell considers the self-weight of the slabs and metallic beams of the experimental apparatus. The slabs were submitted to loadings at intervals of 50 kN, with constant monitoring of deformations and displacements. As the deformations indicated a possible failure, load intervals were reduced to refine the data obtained, improving the analysis of the structural element behavior.

The failure load calculations and the predicted failure mode were based on NBR 6118 [11] for conventional studs are exposed in Table 1.

Table 1: Characteristics, load and failure mode.

Slabs	d (mm)	h (mm)	ρ (%)	f_c (MPa)	P_u (kN)	P_{calc} (kN)	P_u/P_{calc} (kN)	Failure mode	
								Predicted	Real
LRef-AC	116	155	1.65	47.2	665	632	1.05	EP**	EP**
L-5-6	113	153	1.73	44.3	500	610	0.82	EP**	IP*
L-5-13	115	155	1.67	42.0	660	602	1.10	EP**	EP**
LRef-AC-I	113	154	1.73	46.5	551	478	1.15	IP*	IP*
L-5-6-I	113	154	1.73	46.7	450	479	0.94	IP*	IP*
L-5-13-I	116	157	1.65	46.4	525	485	1.08	IP*	IP*
LRef	116	155	1.65	47.2	320	310	1.03	Punching	Punching

*IP: Internal Punching (in the region of shear reinforcement) according to NBR 6118 [11]. **EP: External Punching (after the region of the shear reinforcement) according to NBR 6118 [11]

All slabs analyzed showed a failure load higher than the design load defined by NBR 6118 [11], except for the slabs that used only 6 layers of anti-cracking pins (L-5-6 and L-5-6-I). Only the slab L-5-6 did not present failure mode with the normative prediction.

Compared to the reference slab LRef the load gain with the use of conventional shear reinforcement was 107% for LRef-AC and 72% for LRef-AC-I. With the use of the proposed reinforcement the gain was 106% for L-5-13 and 64% for L-5-13-I.

When performing the comparison of the reinforcement models with their respective reference slabs, despite not reaching higher loads, the slabs with internal shear reinforcement yielded a capacity very similar to the slabs with external reinforcement. The difference in load was less than 1% between LRef-AC and L-5-13 and 4% between LRef-AC-I and L-5-13-I.

It is possible to identify the interference of the number of layers of anti-cracking pins in the strength and failure mode, in such a way that the slabs with fewer layers have the lowest failure loads of the slabs with shear reinforcement. This behavior is valid both for slabs with external failure prediction, as for slabs with internal failure prediction.

3.2 Vertical displacement

The vertical displacements were monitored by 13 LVDT's in only one quadrant of the slabs in directions perpendicular to each other and centered, as shown in Figure 13. LVDTs were installed in the ties in order to subtract their displacements, obtaining the real displacement of the slabs.
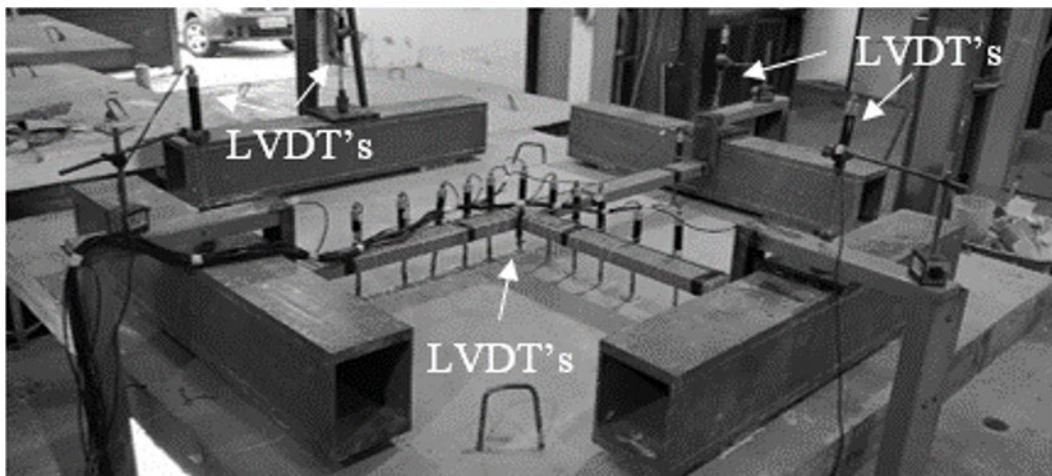
Figure 13: Positioning of the LVDT's.

In all slabs, the maximum displacement was obtained in the central region (LVDT 1) gradually decreasing as approaching the edges, it was possible to observe a certain symmetry in the displacement in the equidistant perpendicular axes. Figures 14 to 17 show the vertical displacement in different loading ranges.
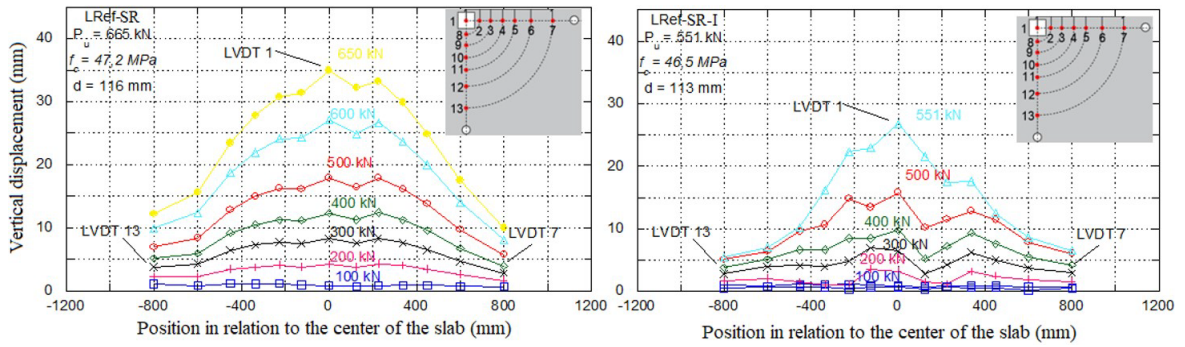
Figure 14: Vertical displacement of slabs LRef-SR and LRef-SR-I.
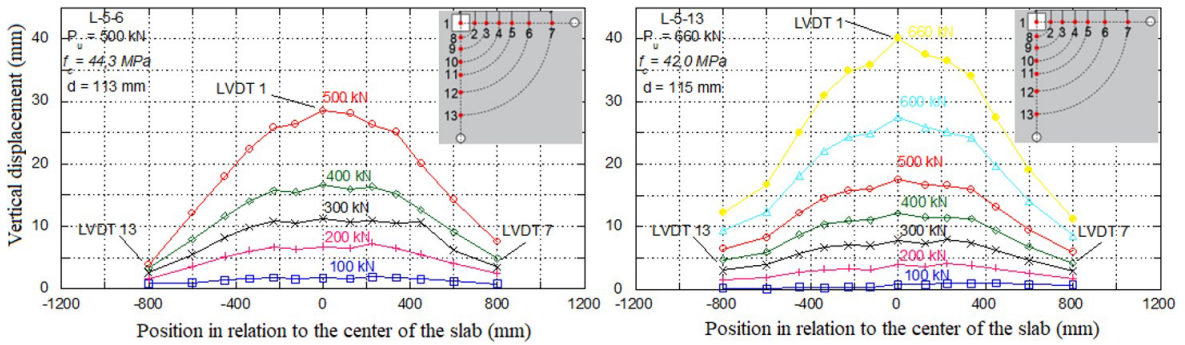
Figure 15: Vertical displacement of slabs L-5-6 and L-5-13.
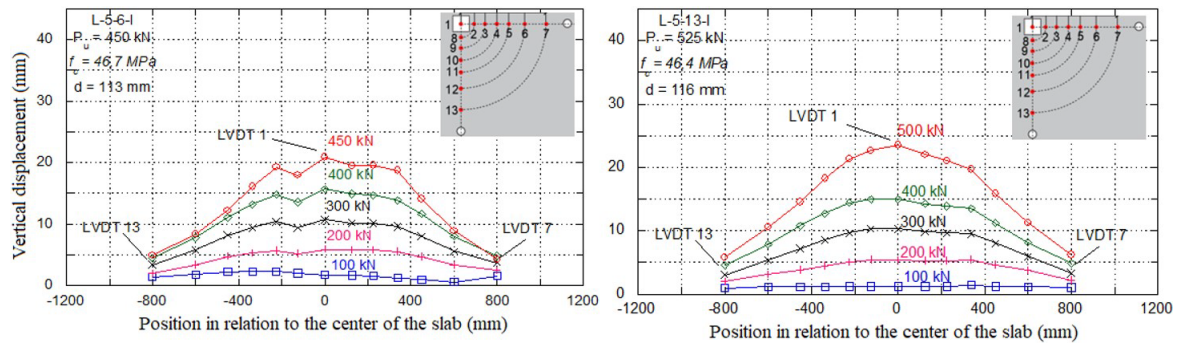
Figure 16: Vertical displacement of slabs L-5-6-I and L-5-13-I.
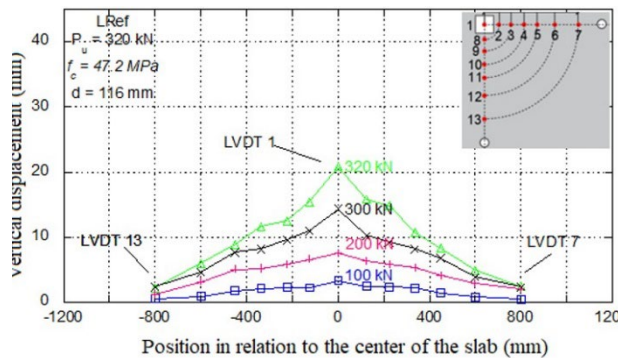
Figure 17: Vertical displacement of slabs LRef.

Rev. IBRACON Estrut. Mater., vol. 16, no. 3, e16305, 2023

8/15

Analyzing the displacement in the loading range of 300 kN, a load close to the failure of the LRef slab, an increase in the rigidity of the slabs with shear reinforcement is observed. This increase was in the order of 50% (L-5-6-I, L-5-13-I, L-5-6) and 47% (L-5-13, LRef-SR, Lref-SR-I).

Regarding the maximum displacement, the slabs that showed greater ductility with higher displacements were: L-5-13-I with external failure prediction, and LRef-SR-I with internal failure prediction.

3.3 Strain of the flexural reinforcement

Figure 18 shows the mapping of the yield radius of the flexural reinforcement, it used data from strain gauges (SG) installed in the most loaded bars (outermost). The analysis area is divided into 5 bands delimited by the position of the SG's, the radii have the following distances from the center of the column: 6 cm, 25 cm, 37 cm, 49 cm and 85 cm.
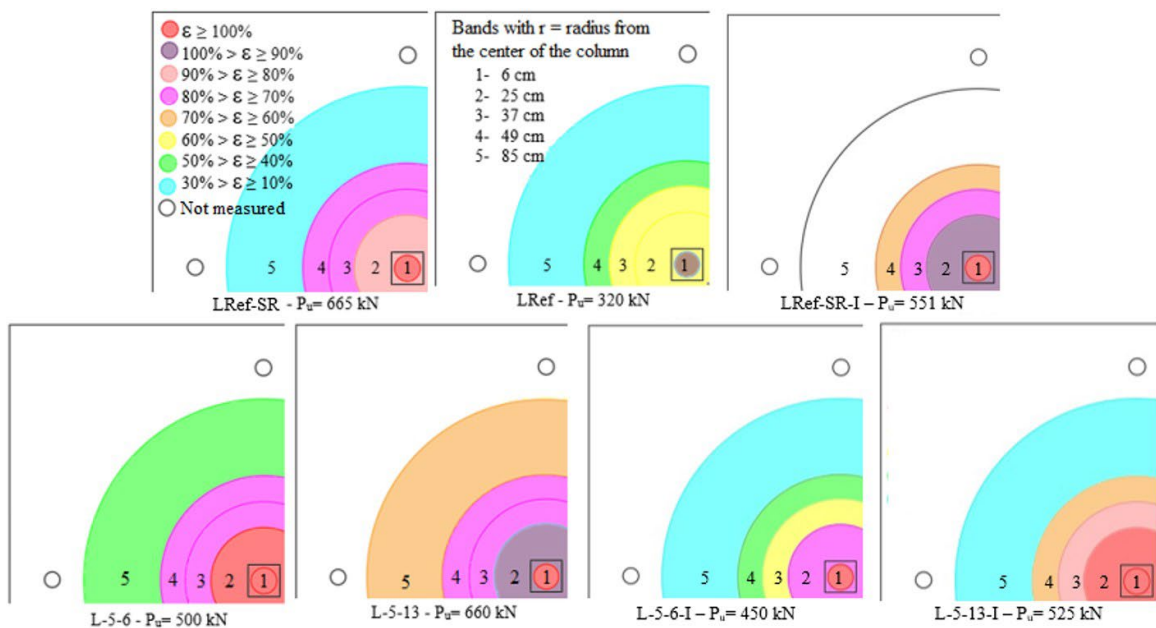
Figure 18: Mapping the yield radius.

In all slabs, it is possible to observe the yield of the reinforcement in the central region (column region, with the exception of the reference slab LRef that showed in this same region strain above 90% of the yield strain.

Analyzing the slabs with internal failure prediction (LRef-SR-I, L-5-6-I and L-5-13-I), it can be seen that there was a greater load distribution in the slab L-5-13-I increasing the yield radius until the second range. Slab L-5-6-I, range 2, showed strain between 80% and 70% while the same range in reference slab LRef-SR-I showed strain between 90% and 100%.

Regarding the slabs of external failure prediction, the slab L-5-13 had greater load distribution, its yield radius was concentrated in the first range, but the fifth and the final range of analysis showed the highest strain among the slabs analyzed with a strain between 60% and 70% of the yield strain characteristic.

This behavior shows the marked ductility of this slab, which was visually verified during the failure of this model.

3.4 Strain of the shear reinforcement

The shear reinforcement strains were measured with electrical resistance strain gauges (SG) in all layers of the same stud line.

Figure 19 shows the shear reinforcement strains of the LRef-SR and LRef-SR-I slab, and indicate higher strains in the layers closest (SG's 1 and 2) to the loaded region (column).
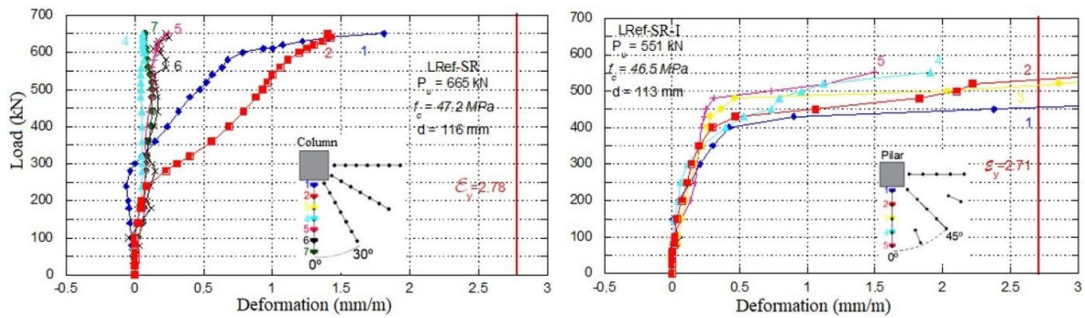
Figure 19: Strain of shear reinforcement, slabs LRef-SR and LRef-SR-I.

The LRef-SR slab showed external failure surface to the region of the shear reinforcement, the late horizontality of the curves demonstrate this behavior, while the LRef-SR-I slab shows horizontality at lower loads and strains that reached the yield strain characteristic of steel. This behavior indicates an internal failure, since the crossing of the failure surface line by a layer of shear reinforcement causes its yielding.

Figure 20 shows the shear strains of the slabs L-5-6 and L-5-13.
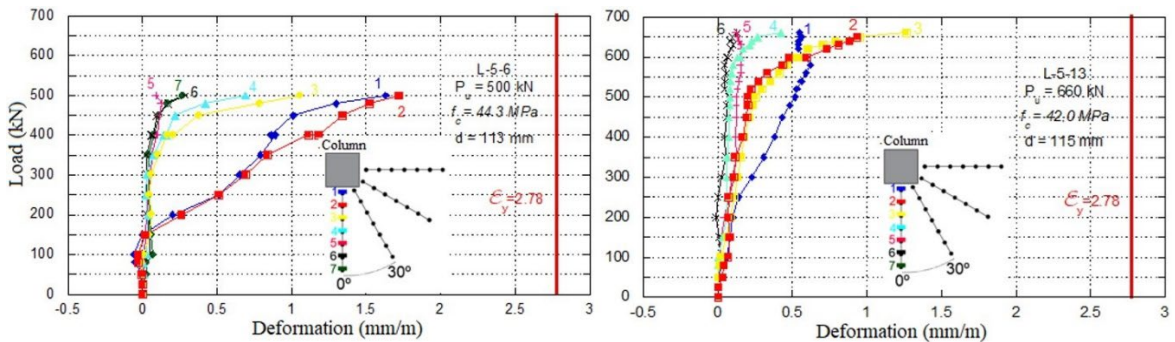
Figure 20: Strain of the shear reinforcement of slab L-5-6 and L-5-13.

The slab L-5-6 presented higher strains in the layers closest to the column region (layers 1 and 2), and no layer reached the characteristic yield strain. The maximum strain recorded reached approximately 62% of the yield strain obtained in the characterization test.

The slab L-5-13 presents lower strains than LRef-AC, and in order of 35% of the yield strain. Layer 1 showed greater strain at initial loads, and at 85% of the final load the curve shows a stress relief, which may have occurred due to the loss of the SG gauging capacity. The horizontality of the curves in the failure loads demonstrate a tendency for the reinforcement to yield.

The shear reinforcement strains of the slabs L5-6-I and L-5-13-I are presented in Figure 21.
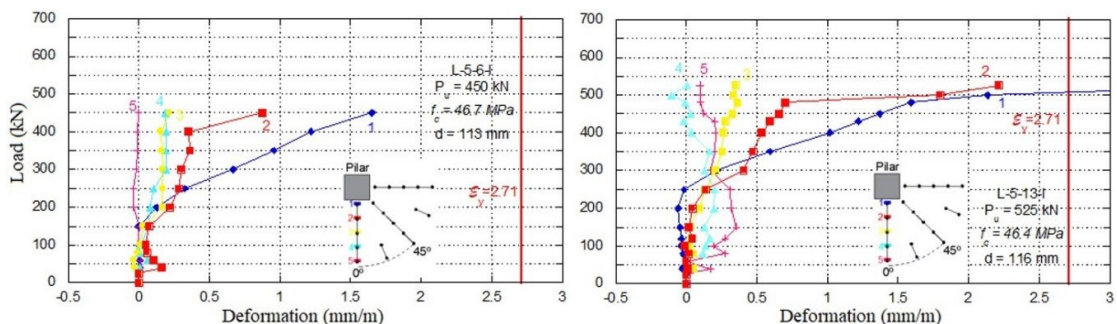
Figure 21: Strain of the shear reinforcement slab L-5-6-I and L-5-13-I.

The slab L-5-6-I has shear reinforcement strains smaller than the characteristic yield strain, layers 1 and 2 had the largest strains, showing the appearance of cracks in this region. Despite not reaching the yield strain, the horizontality of the curves of these layers indicates that the failure surface passed through these layers, which was visually verified in the slab.

The slab L-5-13-I showed strains that reached the yield strain, the most strained layers are the two closest to the column, indicating that the failure surface passed through them, which was also visually observed in the slab.

3.5 Strain on the anti-cracking pins

All the one line anti-cracking pins were instrumented, there was no characteristic yield strain in any case, but as in the shear reinforcement there was a horizontality on the strain curves of the ultimate loads. It is possible to observe that the largest strains occurred in the pins closest to the column region, decreasing linearly as they move away (Figures 22 and 23).
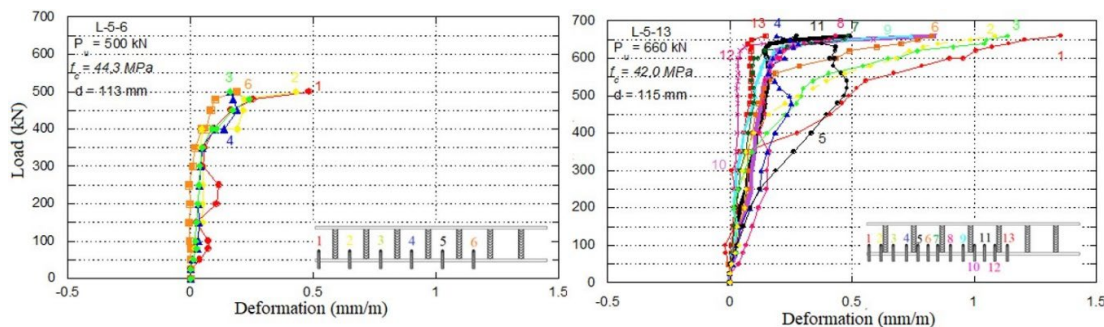
Figure 22: Strain of the anti-cracking pins of slabs L-5-6 and L-5-13.
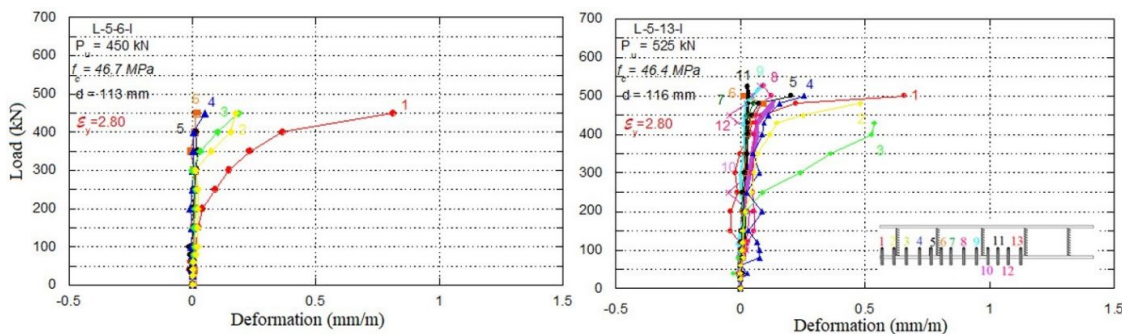
Figure 23: Strain of the anti-cracking pins of slabs L-5-6-I and L-5-13-I.

The maximum strains recorded were at the pin closest to the column with 47% (L-5-13) and 25% (L-5-13-I) of the yield strain. The stresses are more concentrated in the pins as the load increases.

In slab L-5-13-I it can be seen that the most distant pins experience very little strains, which may even reduce the amount of pins in this slab, unlike the slab L-5-13 in which even the most distant pins have larger strains with horizontal behavior in the ultimate loads.

3.6 Comparison of the experimental failure load with loads predicted in analytical models.

For the purpose of comparative analysis between the slabs tested with codes and standards, it was decided to evaluate the failure load with the results theoretically obtained by such normative instructions. Comparative data are shown in Table 2.

One must note that there is no normative forecast for the internal stud-type shear reinforcement model proposed in this study. The following codes were used for this analysis: ACI 318 [13], Eurocode 2 [14], NBR 6118 [11].

The ACI 318 [13] code establishes, for the design of slabs subject to punching, the application of Equation 1:

$$V_n = V_c + V_s \qquad (1)$$

Where "Vn" is the shear strength, constituted by the contribution portion of the concrete (Vc) and the contribution portion of the steel of the shear reinforcement (Vs). For slabs without shear reinforcement, the failure load at the punch of the slab-column connection must be equal to the smallest result obtained with the application of Equations 2 to 4:

$$V_c = 0{,}33\lambda_s\lambda\sqrt{f_c'} \tag{2}$$

$$V_c = 0{,}17\left(1+\frac{2}{\beta}\right)\lambda_s\lambda\sqrt{f_c'} \tag{3}$$

$$V_c = 0{,}083\left(2+\frac{\alpha_s d}{b_0}\right)\lambda_s\lambda\sqrt{f_c'} \tag{4}$$

For slabs with shear reinforcement, the calculation of the resistant portion of concrete V_c for slabs with reinforcement, composed of stirrups must be done in the two control perimeters by Equation 5:

$$V_c = 0{,}17\lambda_s\lambda\sqrt{f_c'} \tag{5}$$

Concerning the slabs with reinforcement composed of studs, the shear force at the first critical perimeter must be equal to the lowest value obtained by Equations 6 to 8:

$$V_c = 0{,}25\lambda_s\lambda\sqrt{f_c'} \tag{6}$$

$$V_c = \left(0{,}17+\frac{0{,}33}{\beta}\right)\lambda_s\lambda\sqrt{f_c'} \tag{7}$$

$$V_c = \left(0{,}17+\frac{0{,}083\alpha_s d}{b_0}\right)\lambda_s\lambda\sqrt{f_c'} \tag{8}$$

Figure 24 shows the control perimeters established by ACI 318 [13].
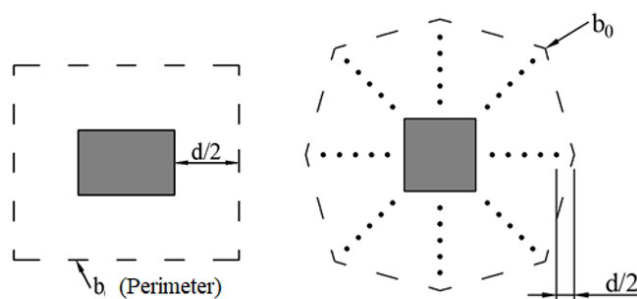
Figure 24: Adapted ACI 318 [13] control perimeter.

Eurocode 2 [4] recommends, establishing for the proper dimensioning of slabs subject to punching, that the maximum shear force must not exceed the maximum shear force capacity according to Equations 9 to 11.

$$V_{Ed} \leq V_{Rd} \tag{9}$$

$$V_{Ed} = \beta\frac{F_{sd}}{u_0 d} \tag{10}$$

Rev. IBRACON Estrut. Mater., vol. 16, no. 3, e16305, 2023

12/15

$$V_{Rd,max} = 0,4(1 - \tfrac{f_{ck}}{250})f_{cd}u_0 d \qquad (11)$$

For slabs without shear reinforcement, only the contribution portion of the concrete must be considered in the calculation of the punching ultimate load. Equation 12 calculates the shear force capacity from concrete.

$$V_{Rd,c} = 0,18k(100\rho f_{ck})^{1/3} \geq V_{min} \qquad (12)$$

Where: $V_{min} = 0,035k^{2/3}f_{ck}^{1/2}$

Equations 13 and 14 give the calculation of shear strength in the region with shear reinforcement.

$$V_{Ed} \leq V_{Rd,cs} \qquad (13)$$

$$V_{Rd,cs} = 0,75V_{R,dc} + 1,5\tfrac{d}{s_r}A_{sw}f_{ywd,ef}\left(\tfrac{1}{u_1 d}\right)sen\alpha \qquad (14)$$

Equations 15 and 16 are used to calculate shear strength for regions external to the shear reinforcement.

$$v_{Ed} \leq v_{Rdc,ext} \qquad (15)$$

$$V_{Rd,cs,ext} = V_{Rd,c}\mu_{out}d \qquad (16)$$

Figure 25 details the control perimeter for this analysis.
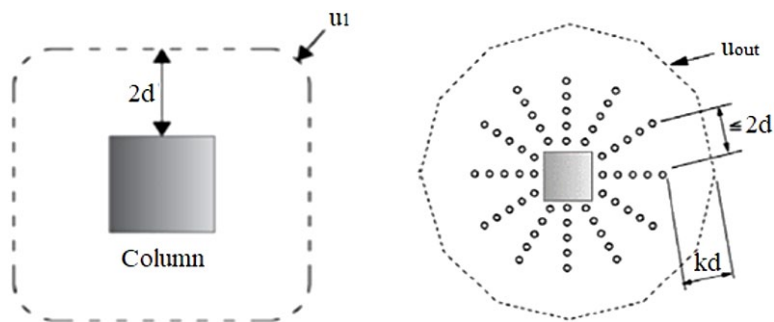
Figure 25: Adapted Eurocode 2 [14] control perimeter.

NBR 6118 [11] establishes that for symmetrical loading in internal columns, the stress on critical surfaces C and C' is calculated by Equation 17:

$$\tau_{sd} = \tfrac{F_{sd}}{\mu d} \qquad (17)$$

To avoid cracking by diagonal compression of the concrete on the critical surface C, the verification in flat slabs with or without shear reinforcement must be solved by Equation 18.

$$\tau_{sd} \leq \tau_{Rd2} = 0,27\alpha_v f_{cd} \qquad (18)$$

To verify the shear stress acting on the critical surface C' in flat slabs without shear reinforcement, Equation 19 is used.

$$\tau_{sd} \leq \tau_{Rd1} = 0,13(1 + \sqrt{\frac{20}{d}})(100\rho f_{ck})^{1/3} \tag{19}$$

To verify the shear stress acting on the critical surface C' in flat slabs with shear reinforcement, Equation 20 is used.

$$\tau_{sd} \leq \tau_{Rd1} = 0,13(1 + \sqrt{\frac{20}{d}})(100\rho f_{ck})^{1/3} + 1,5\frac{d}{s_r}\frac{A_{sw}f_{ywd}sen\alpha}{\mu d} \tag{20}$$

The control perimeters established by NBR 6118 [11] are shown in Figure 26.
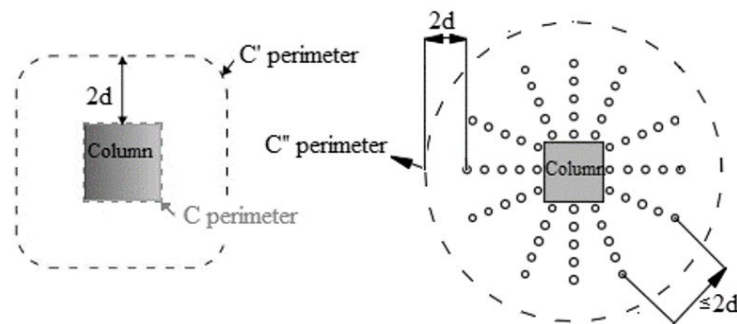
Figure 26: Adapted NBR 6118 [11] control perimeter.

The comparison of the experimental results with that predicted by the calculation according to NBR 6118 [11] is presented in Table 2. Regarding the result (Pu/Pcalc), it is possible to observe that the LRef, LRef-SR, and L5-13 slabs presented a failure load greater than that calculated with this code formulation. The others slabs cracked with a load lower than the predicted, ranging between 8% and 18% lower.

Table 2: Comparison of experimental results with codes specifications.

Slabs	P_u kN	ACI 318 [13]				Eurocode 2 [14]				NBR 6118 [11]			
		P_{calc} kN	P_u/P_{calc}	b0 mm	b0sr mm	P_{calc} kN	P_u/P_{calc}	u_1 mm	u_{out} mm	P_{calc} kN	P_u/P_{calc}	C' mm	C'' mm
LRef-SR	665	426	1.56	1064	3144	691	0.96	2080	3874	632	1.05	2080	4244
L-5-6	500	401	1.25	1052	3134	656	0.76	2020	3836	610	0.82	2020	4235
L-5-13	660	398	1.66	1060	3140	655	1.01	2045	3854	602	1.10	2045	4231
LRef-SR-I	551	398	1.39	1052	3134	404	1.36	2020	3836	478	1.15	2020	4235
L-5-6-I	450	397	1.13	1052	3134	405	1.11	2020	3836	479	0.94	2020	4235
L-5-13-I	525	409	1.28	1064	3144	419	1.25	2080	3874	485	1.08	2080	4244
LRef	320	254	1.14	1064	-	371	0.86	2080	-	310	1.03	2080	-

Compared to ACI 318 [13], no slab presented a failure load lower than that predicted by the code; Pu/Pcalc results range from 13% (L-5-6-I) to 66% (L-5-13).

When comparing with Eurocode 2 [14], the L-5-13 and LRef-SR slabs presented a Pu practically equal to Pcalc, while the slabs LRef and L-5-6 presented a Pu lower than Pcalc, varying between 14% and 24% respectively, thus the obtained results (Pu/Pcalc) are against security. All slabs predicted to failure internally reached a failure load greater than the design load. The control perimeter 1.5d away from the last layer of shear reinforcement was adopted.

4 CONCLUSION

The use of internal stud-type shear reinforcement looks promising, since the increase in strength of the slab without shear reinforcement reached the order of 106% in L-5-13 and 64% in L-5-13-I. These same slabs compared to the

Rev. IBRACON Estrut. Mater., vol. 16, no. 3, e16305, 2023

14/15

models that used standardized studs showed very close failure loads, L-5-13 less than 1% lower than LRef-AC and L-5-13-I 5% lower than LRef-AC-I.

The data points to a direct relationship between the amount of anti-cracking pins and the capacity of the structural element. The smaller the spacing between pins in the 2d control perimeter the greater the capacity and ductility.

The anti-cracking pins in the layers farthest from the column in the slabs with internal failure prediction, presented small strains, indicating that the positioning of the pins in slabs with this failure prediction can be installed covering a smaller region, different from the 2d control perimeter proposed in this study.

The pins fulfilled the function of preventing the development of cracks tangential to the base of the studs as observed in previous research, avoiding the failure designated as delamination.

Regarding normative specifications, further studies are necessary to develop na adequate design model that can describe the behavior of the proposed reinforcement.

About the on-site assembly process, the proposed model shows to be efficient given the ease of assembly of the structural components and the guarantee of the design specifications, such as the spacing between the flexural reinforcement and the perfect radial distribution of the shear reinforcement lines, something that proved to be complicated for slabs with conventional studs.

ACKNOWLEDGEMENTS

5 REFERENCES

[1] L. M. Trautwein, T. N. Bittencourt, R. B. Gomes, and Bella, J.C.D., "Punching strength of flat slabs with unbraced shear reinforcement," *ACI Struct. J.*, vol. 108, pp. 197–205, 2011.

[2] R. B. Gomes, "Punching resistance of reinforced concrete flat slabs with shear reinforcement," Ph.D. dissertation, Polytech. Cent. London, London, 1991.

[3] C. E. Broms, "Elimination of flat plate punching failure mode," *ACI Struct. J.*, vol. 97, no. 1, pp. 94–101, Jan-Feb 2000.

[4] J. Hegger, A. G. Sherif, D. Kueres, and C. Siburg, "Efficiency of various punching shear reinforcement systems for flat slabs," *ACI Struct. J.*, vol. 114, no. 3, pp. 631–642, 2017.

[5] F. Samadian, "Shear reinforcement against punching in reinforced concrete flat slabs," *Struct. Eng.*, vol. 79, no. 10, pp. 24–31, 2001.

[6] K. Pilakoutas and X. Li, "Alternative shear reinforcement for reinforced concrete flat slabs," *J. Struct. Eng.*, vol. 129, no. 9, pp. 1164–1172, 2003.

[7] S. Lips, M. Fernández Ruiz, and A. Muttoni, "Experimental investigation on punching strength and deformation capacity of shear-reinforced slabs," *ACI Struct. J.*, vol. 109, no. 6, pp. 889–900, 2012.

[8] M. P. Ferreira, R. N. M. Barros, M. J. M. Pereira Filho, L. S. Tapajós, and F. S. Quaresma, "One-way shear resistance of RC members with unconnected stirrups," *Lat. Am. J. Solids Struct.*, vol. 13, no. 15, pp. 2970–2990, 2016.

[9] M. A. S. Andrade, "Punção em lajes cogumelo – estudo do posicionamento da armadura de cisalhamento em relação à armadura de flexão," M.S. thesis, Esc. Eng. Civ., UFG, Goiânia, 1999.

[10] L. M. Trautwein, "Punção em lajes cogumelo de concreto armado: análise experimental e numérica," Ph.D. dissertation, Dep. Eng. Estru. Fund., Esc. Politéc., Univ. São Paulo, 2006, 350p.

[11] Associação Brasileira de Normas Técnicas, *Projeto de Estruturas de Concreto - Procedimento*, ABNT NBR 6118, 2014.

[12] M. G. Marques, E. A. P. Liberati, R. B. Gomes, and L. M. Trautwein, "Study of failure mode of reinforced concrete flat slabs with openings and studs," *ACI Struct. J.*, vol. 117, no. 4, pp. 39–48, 2020.

[13] American Concrete Institute, *Building Code Requirments for Structural Concrete and Commentary (ACI 318R-11)*, ACI 318-19, 2019.

[14] European Committee for Standardization, *Eurocode 2, Design of Concrete Structures – Part 1-1 General Rules and Rules for Buildings*, CEN EN 1992-1-1:2004/prA1:2013, 2014.

Author contributions: Contribution description of each co-author for the study. LMT: conceptualization, funding acquisition, data curation, supervision, writing; JPV: experimental tests, data curation; RBG and LCA: data curation, formal analysis.

Editors: Mauro Real, Mario Pimentel.